Effects of Air Film Cooling on Rotating Detonation Engine

Kevin Y. Cho, Scott L. Chriss, John L. Hoke
Innovative Scientific Solution Inc.
Dayton, OH, USA

Adam T. Holley, S. Alexander Schumaker
Air Force Research Laboratory
Wright-Patterson Air Force Base, OH, USA

1 Introduction

The potential for rotating detonation engines (RDEs) to significantly improve specific impulse through increased thermal efficiency arises from the increase in stagnation pressure achieved across the detonation wave. The prospect of this increased efficiency has led to widespread research on these devices, but significant technical challenges remain. To date, high heat loads in RDEs remain a key obstacle for long duration testing and practical flight. The current study aims to gain deeper understanding of the air film cooling in RDEs. The primary objective is to identify key design features that affect operability and cooling effectiveness using a limited run time. The experiment will be conducted on a modular outerbody with replaceable cooling liner with different cooling hole geometries.

2 Experimental Setup

This research was conducted at the Detonation Engine Research facility (DERF) at the Air Force Research Laboratory (AFRL), Dayton OH. Several film cooled RDE outer body liners were manufactured out of 304 stainless steel for testing in a laboratory scale RDE operating on H_2-air. The RDE utilized in the present research was an axial air injected 6-inch nominal diameter, with a channel width of 1.63 cm (0.64 inch) and an outer diameter of 17.1 cm (6.74 inch), and an axial length of 15.2 cm (6 inch). The RDE used a jet in cross flow inner diameter injection scheme with an air injection area ratio of 0.33, an aerospike plug nozzle with area ratio of 0.66 and 1.0, and a heat sink center body. The fuel plate had 120 × 0.89 mm (0.035 inch) diameter injection holes, with injection taking place at the throat of the air inlet.

Four liners with cooling holes and one blank were manufactured. Two liners were machined traditionally with round holes, while the other two were 3D printed with shaped diverging holes. The two liners with cylindrical holes had approximately equivalent total area ratios, with equivalent row and circumferential spacing relative to the hole diameters. All four liners were made of 304 stainless steel, had a thickness of 2.54 mm (0.1 inch), and had an injection angle of 30°. Two film cooled liners with round holes used EDM manufacturing. The two shaped diverging holes were directly 3D printed.

Correspondence to: kycho25@gmail.com

The printed holes were about 50 μm (0.002 inch) smaller than originally designed. All dimensions are summarized in Table 1. Testing utilized a sweep of equivalence ratios from 0.5 to 1.25 with an uncertainty of ± 0.05, all with an air mass flow rate of 0.91 and 1.36 kg/s (2 lbm/s and 3 lbm/s), with an uncertainty of ±0.02kg/s (±0.05 lbm/s). These supply conditions led to blowing ratios between 0 – 8. All test conditions are summarized in Table 2.

Table 1: Liner Dimensions and Instrumentation

	Liner-1	Liner-2	v2.7	v2.8
Hole Diameter	1.19 mm (0.047 in)	0.635 mm (0.025 in)	0.53×0.53 mm (0.021×0.021 in)	0.61×0.61 mm (0.024×0.024 in)
Number of Holes	378	1300	1300	2340
Total Area	4.23 mm^2 (0.656 in^2)	4.12 mm^2 (0.638 in^2)	3.70 mm^2 (0.573 in^2)	8.71 mm^2 (1.35 in^2)
Circumference Pitch	18° (16.7 D)	6.9° (16.3 D)	6.9°(16.9 D)	4° (8.7 D)
Vertical Pitch	6.38 mm (0.259 in) (7.7 D)	4.95 mm (0.195 in) (7.7 D)	4.95 mm (0.195 in) (8.1 D)	5.08 mm (0.2 in) (7.4 D)
TC Placement	2.29, 8.38, 14.2 cm (0.9, 3.3, 5.6 in)	2.03, 7.37, 12.7 cm (0.8, 2.9, 5.0 in)	2.03, 7.37 cm (0.8, 2.9 in)	2.29, 6.60 cm (0.9, 2.6 in)
HS Kulite Placement	2.41, 12.6 cm (0.95, 4.95 in)	2.41, 12.6 cm (0.95, 4.95 in)	2.41, 12.6 cm (0.95, 4.95 in)	2.41, 12.6 cm (0.95, 4.95 in)

Table 2: Summary of test conditions

Main air mass flowrate	0.91 kg/s, 1.36 kg/s (2 lbm/s, 3 lbm/s)
Cooling air mass flowrate (percent of total)	0%, 10%, 20%, 30%, 40%
Equivalence ratios (local, excluding cooling air)	0.5, 0.75, 1.0, 1.25

Cooling air was supplied with eight 12.7 mm (0.5 inch) tubes supplying cooling air to the outer diameter of the manifold. After each test run the hardware was air cooled to uniform temperatures between 27-38 C (80 – 100°F). Unfiltered chemiluminescence looking down the channel was recorded using a Phantom v711 high-speed camera with 200 mm lens, at 50k FPS to confirm operating mode. FLIR SC6810 IR camera with unfiltered 25mm lens was used to view the emission of the outer surface of the liner through a sapphire window. Since the welded thermocouple positions are known, the emission counts can be correlated with the thermocouple data during post-processing to get a 2D temperature profile for each run. The IR camera was operated at 10 Hz.

Before ignition with a pre-detonator, the fuel, oxidizer, and cooling air feed pressures were stabilized. Uncooled test duration was for 2 seconds and cooled test duration was for 5 seconds. Figure 1 shows the entire assembly of the engine tested.

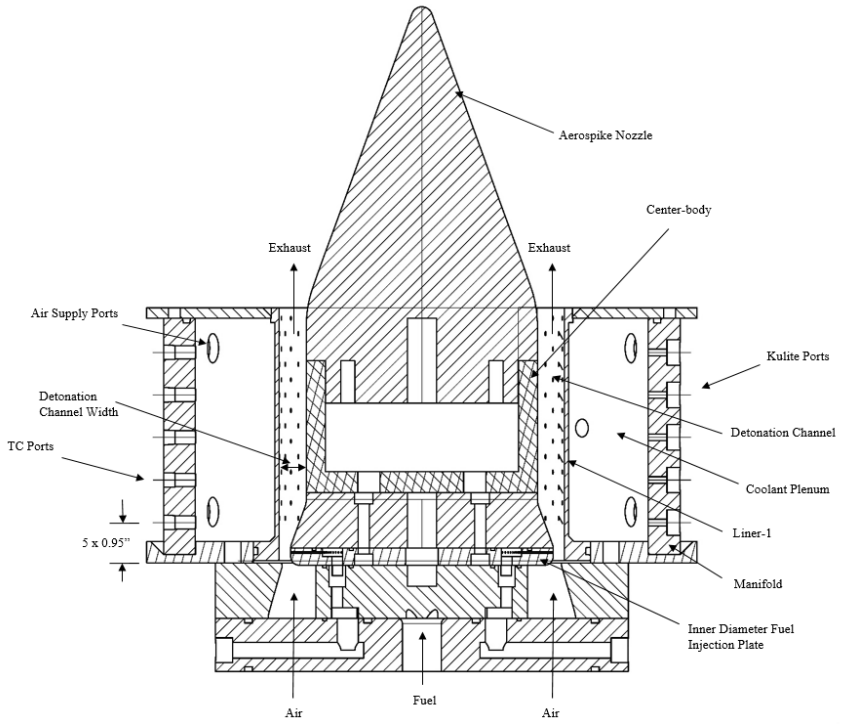

Figure 1: Engine Assembly

3 Results and Discussion

For each test condition, at least three tests were performed. The unfiltered high speed camera pointing down the channel was used to determine the detonation wave mode. In a 'stable' detonation wave mode, 1 or 2 wave laps the channel consistently and repeatedly. In an 'unstable' detonation wave mode, the direction, number of waves keep switching during the run (typically multiple times in less than 50 ms). This does not mean there are no detonation waves present. The third mode, 'acoustic/deflagration' consists of random acoustic waves and deflagration, with little to no presence of detonation waves.

Every good test was ranked according to the detonation mode: stable 1, unstable 0.5, and acoustic/deflagration 0. For each test condition, the detonation mode 'score' was averaged to obtain the stability value. The stability value was color mapped and plotted on x and y axis, with x being the equivalence ratio and y being the mass flux ratio. The mass flux ratio is defined here as the mass flux of the cooling air jet divided by the mass flux of the main air through the channel. For the four liners, the stabilities are plotted in Figure 2 – Figure 3.

In general, detonation wave was more stable with less or no cooling air. This makes sense because the normal RDE is known to operate well in these conditions. The exception was liner v2.8 where it behaved unstably in lower cooling air mass flow rates throughout the equivalence ratio range. A possible explanation is weakening of the detonation due to the 'porous' wall when cooling air is not pressurized enough. Since v2.8 had the largest total cooling hole area, this effect will be amplified the most. Conversely, liner v2.8 fared better in higher cooling air mass flowrates than other liners. A possible explanation is the holes no longer become 'porous' with more pressurization and flow, and the cooling air jet disturbs the fuel and air mixture less from reduced jet velocity.

Another anomaly that was observed was equivalence ratio 0.5 case being stable for high cooling air flow rates in liner 1 and 2. A caveat is the chemiluminescence observed with the high speed camera

was relatively low in these conditions and liners. Repetition of chemiluminescence pulses were observed in a few distinct spots. They were not seen making a lap around the channel, but they were repeatable so they were considered to be a stable detonation wave. Further investigation with the camera looking straighter down the channel with a mirror or a deeper analysis of the high speed pressure data in the main air supply manifold may be needed to rule out these conditions.

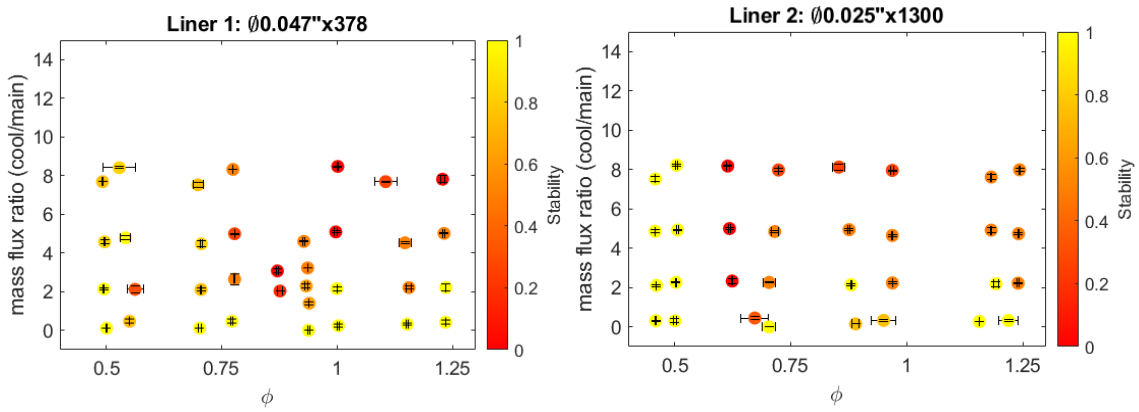

Figure 2: Left: Stability (higher is more stable detonation) of liner 1. Right: Stability (higher is more stable detonation) of liner 2. Error bars indicate ±standard deviation.

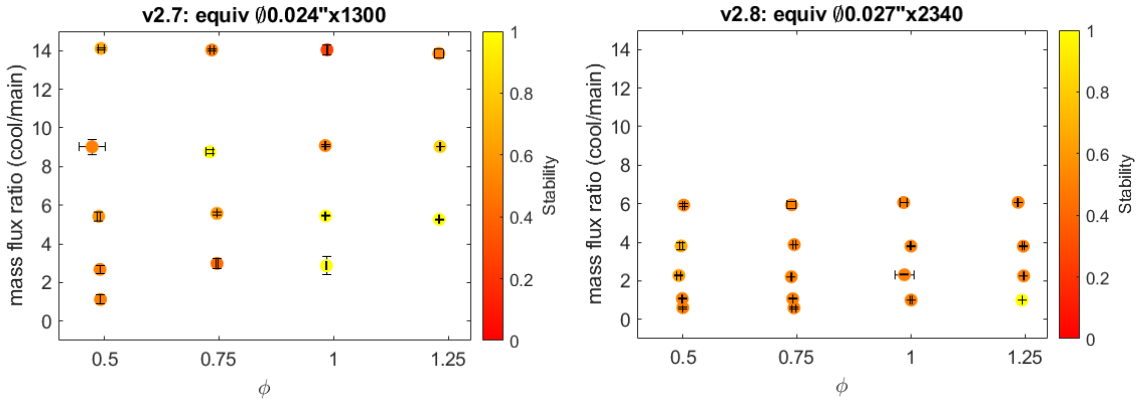

Figure 3: Left: Stability (higher is more stable detonation) of liner v2.7. Right: Stability (higher is more stable detonation) of liner v2.8. Error bars indicate ±standard deviation.

In order to compare the liner temperature, an equivalence ratio that had the most stable detonation modes for the four liners was chosen. This is because the detonation mode has a significant impact on the heat release. To compare the film cooling effectiveness of the liners, variability from the detonation mode needed to be minimized. Equivalence ratio of 1 was chosen, and test cases that were acoustic/deflagration were disregarded for this comparison. Test with a short duration were also disregarded. The maximum thermocouple reading out of 2-3 thermocouples at the end of the test ($t_{ignition}$ + 5 seconds) was chosen to be compared. Figure 4 shows a plot of the maximum thermocouple reading at the end of the 5 second run for all four liners at equivalence ratio 1. The temperature is plotted against the cooling air bypass ratio, and the marker color map displays the little variations of the equivalence ratio. Note the markers for liner 1 are shaped similarly (square and diamond), markers for liner 2 are shaped similarly (triangle pointing up or down), and markers for liner v2.7 and v2.8 are shaped similarly (pentagram and hexagram).

As expected, with more cooling air, the maximum temperature decreases. At lower bypass ratios of 10 and 20%, 1.36 kg/s (3 lbm/s) main air mass flowrates seem to have higher temperatures for liner 1 and liner 2 than 0.91 kg/s (2 lbm/s). This makes sense since higher main air mass flowrates creates higher channel pressure and higher detonation temperature. This difference collapses at 30% bypass ratio. A possible explanation is the cooling air creates a good film at 30% which negates the temperature rise due to increased channel pressure. Liner v2.7, which has the same hole pattern and similar hole size as liner 2, has similar maximum temperature as liner 2 for the range of bypass ratios. This indicates that the shaped diverging holes have miniscule effect on the cooling effectiveness.

The maximum temperature of liner 1, liner 2, and liner v2.7 follow in a very close inverse linear relationship with cooling air bypass ratio. This may signify the total cooling hole area as the most contributing driver in film cooling effectiveness in RDEs. To add to this argument, liner v2.8, which has double the amount of total area, sits far cooler in Figure 4. Although cooling air bypass ratio of 10% was disregarded due to poor stability, 20%, 30%, 40% temperatures follow a very linear trend. In fact, the maximum temperature of liner v2.8 is almost lower by 100 C, which is significant. Unfortunate experiment design flaw is v2.8 has different total area, different number of holes, and are shaped differently, so it is hard to pinpoint the exact contributor to the relatively great film cooling effectiveness. However, judging by comparing the other three liners, the total area seem to be the greatest contributor in film cooling effectiveness in RDEs.

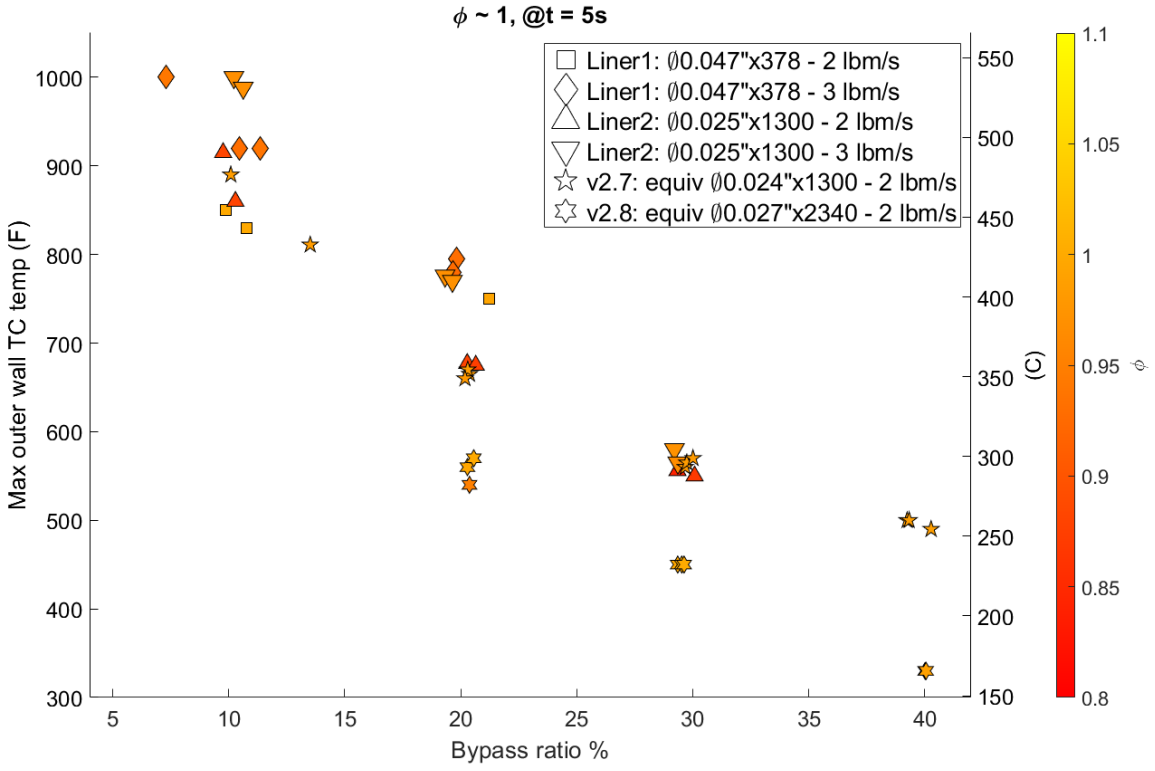

Figure 4: Maximum outer liner thermocouple temperature 5 seconds after ignition plotted as a function of the bypass ratio. The marker color map indicates the slight differences in the equivalence ratio, all from stoichiometric test cases. Note the markers for liner 1 are shaped similarly (square and diamond), markers for liner 2 are shaped similarly (triangle pointing up and down), and markers for liner v2.7 and v2.8 are shaped similarly (pentagram and hexagram).

The unfiltered IR camera was used to obtain uncalibrated IR images. The two axial thermocouple locations were within the view of the IR camera, and they were used to calibrate the images for each run. With the axial locations of the thermocouples and their corresponding pixel locations, the IR data

was calibrated for each test. This data was used to create a curve fit and a function, which typically had an R^2 value of 0.99. This calibration data was used to create images in both F° and C°.

To illustrate the uneven axial temperature, a 1D temperature profiles spanning in the axial direction, not intersecting the cooling holes, were obtained. The axial temperature data is plotted with the maximum temperature at the end of the 5 second run, with different cooling air bypass ratios in Figure 5. It can be observed that even with the increased cooling air flowrate, the upstream side is hotter than the downstream side. Previously, it was hypothesized that the detonation occurs further downstream with more cooling air, but data from FLIR indicated otherwise.

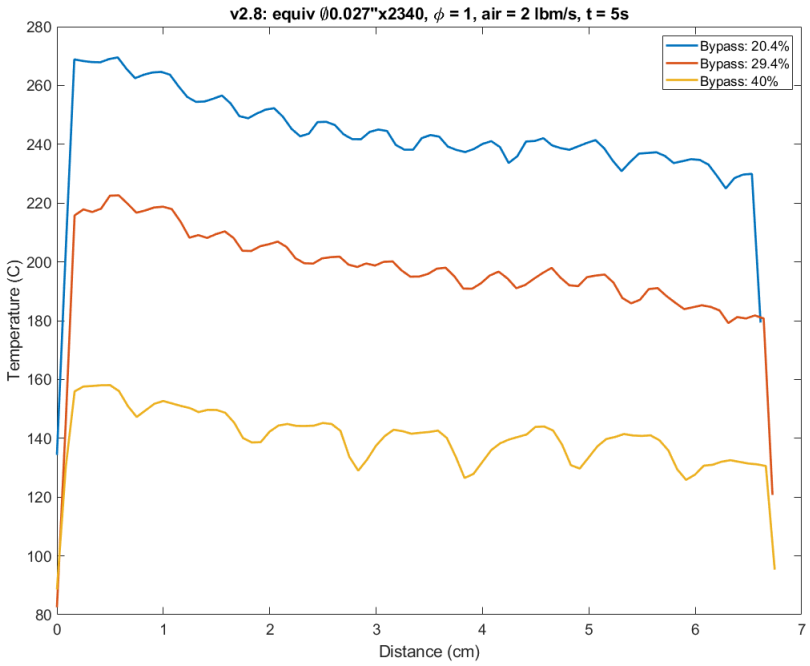

Figure 5: Axial temperature profile at the end of the 5 second run for different bypass ratios. This data is from liner v2.8, $\phi = 1$, main air mass flowrate = 0.91 kg/s (2 lbm/s).